

Geometry and Kinematics of a Convertible's Rear Side Window

Anton Gfrerrer, Johann Lang

*Institute of Geometry, Graz University of Technology
Kopernikusgasse 24, 8010 Graz, Austria
email: gfrerrer@tugraz.at*

Abstract. The design of rear side windows of convertibles (cabriolets) and their motion while being retracted contains interesting geometric and kinematic issues. On the one hand, the space between the door and the rear wheel arch is limited. On the other hand, the window pane has to move through the sealing slit with as little friction as possible. These turn out to be two severe constraints for the window surface and its motion.

In order to allow for the cramped conditions we first compute a spatial motion that assumes prescribed positions and obeys certain side conditions. Having obtained this spatial motion we can replace the given window surface by a kinematic surface which perfectly moves through the sealing slit. Eventually, we construct a set of possible window surfaces. This way the engineer gets a variety of options to choose from.

Key Words: motion interpolation, motion design, kinematic surface, car window design

MSC 2010: 62P30, 68N30, 53A17, 68U07

1. Introduction

Retracting a rear side window of a convertible is particularly intricate. As shown in Figure 1, the motion retracting the window pane is not as simple as a translation or a rotation. There is, in general, too little space for such a simple solution.

A car side window should ideally move ‘*in itself*’ which is to say that all along the motion the window sheet stays on the same surface. Such motions have been harnessed to properly design the geometry and kinematics of a car side window [2], [3]. That approach, however, cannot be applied in our case: Convertibles usually have two doors that are fairly long. Thus, the space between the door and the rear wheel arch is pretty much limited. This is where the rear side window has to be accommodated while retracted. Due to the cramped conditions within the side panel the designer usually prescribes a number of positions S_i^* , $i = 0, \dots, n$,

of the window pane on its path down to the retracted state the way that it does not interfere anywhere.

We have to be aware that, in general, a given surface cannot be moved through a given curve. In terms of the inverse motion we can also put it this way: In general, a given curve cannot be moved across¹ a given surface. If a surface S can be generated by applying a motion μ to a particular curve c then S is called a ‘*kinematic surface*’ or, in more detail, a ‘*kinematic surface with respect to the motion μ* ’. The curve c is called a ‘*generator*’ of the surface S .

Coming back to the problem of our rear side window we have to face the fact that the stylist’s proposal for the rear side window (surface S) will most probably *not* be a kinematic surface generated by the daylight curve c .

This rest of this paper is organized as follows: In Section 2 we construct a suitable window motion μ that interpolates the prescribed positions of S and — at the same time — moves the window with low friction along the sealing slit c . Subsequently, we go on and generate another window sheet S_c that is closely related to the spatial motion μ . It is the great benefit of S_c over S that S_c is a kinematic surface w.r.t. μ generated by the curve c . As opposed to S — it delivers zero friction while being moved through the sealing slit c (Section 3). In Section 4 we construct a whole family of alternative surfaces by means of blending S and S_c . Eventually, the paper will be rounded off by some conclusions (Section 5).



Figure 1: The rear side window of a convertible on its way down into the space between the door and the rear wheel arch.

2. Generating the window motion

The engineer is given (see Figure 2)

- a triangular surface patch S (rear side window pane suggested by the stylist): S has the vertices A, B, C and the boundary curves a (roofline curve), b (front boundary curve) and c (daylight curve).
- a number of single window sheet positions S_i^* , $i = 0, \dots, n$, which have to be assumed in the course of the motion when the window is retracted. We presume that $S_0^* = S$ is

¹The term ‘*moved across*’ means that the curve is always contained in the surface.

the window sheet in its closed position. Moreover, as S has to slide through the sealing slit (the daylight curve c) we can also state that for $i = 0, \dots, n$ the front boundary curve b_i^* and the roofline curve a_i^* of S_i^* meet c in points P_i^* and Q_i^* , respectively. Note that P_0^* is the common point of $b = b_0^*$ and c : $P_0^* = A$. Analogously, Q_0^* is the common point of $a = a_0^*$ and c : $Q_0^* = B$.

As the window has to be retracted completely we have to prescribe the state of S when the window sheet is already below the daylight curve c : We assume that $P_{n-1}^* = Q_{n-1}^*$. This position S_{n-1}^* is called the ‘*vanishing position*’. To sort out odd motions of S , we moreover presume that for $i = 0, \dots, n-2$ the order of the points P_i^*, Q_i^* on c stays the same, whereas for the last position S_n^* , which is already beyond the vanishing position, the order is reversed (Figure 2, right).

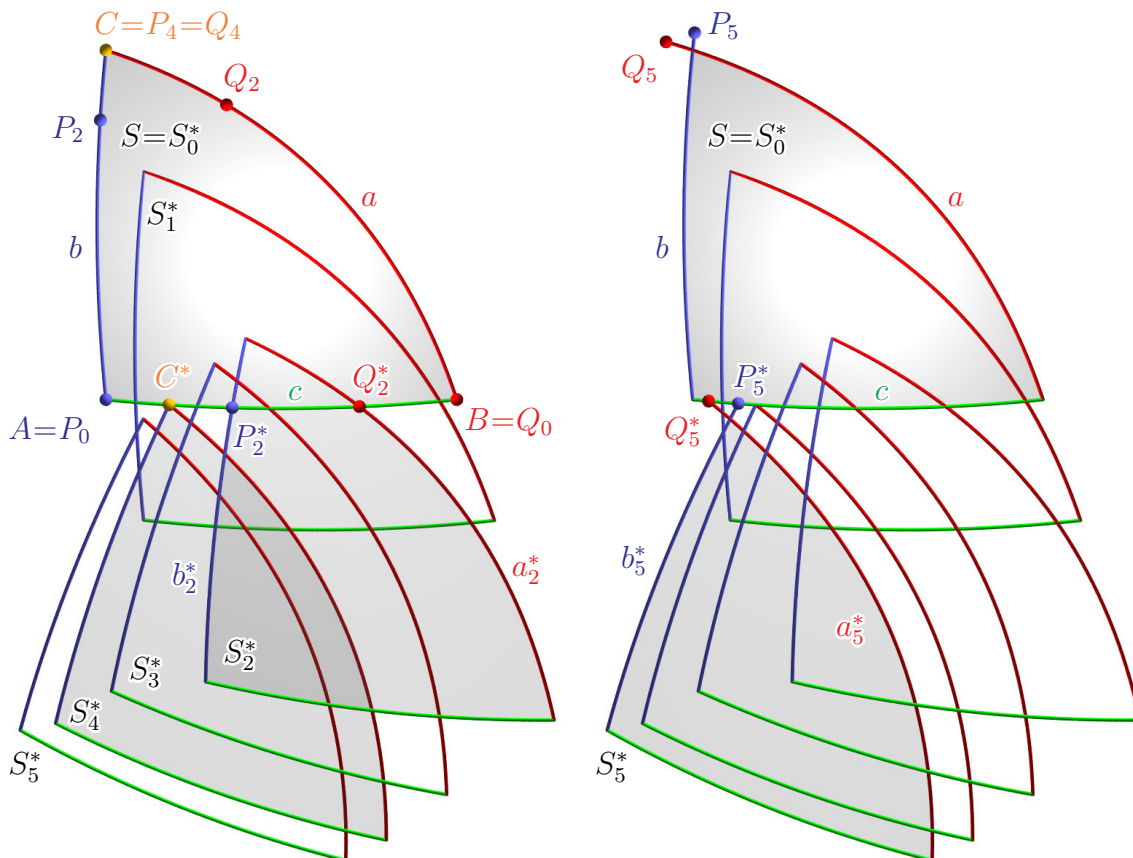


Figure 2: **Left:** Six given positions $S_0^*, S_1^*, S_2^*, S_3^*, S_4^*, S_5^*$ of the the window sheet S . Among them the vanishing position S_4^* . Position S_2^* is displayed together with its points $P_2^* \in b_2^*$ and $Q_2^* \in c_2^*$. The inverse transformation μ_2^{-1} maps the points P_2^* and Q_2^* onto $P_2 \in b$ and $Q_2 \in a$, respectively.

Right: The same input as on the left; here, the last position S_5^* beyond the vanishing position is highlighted. The points $P_5^* \in b_5^*$ and $Q_5^* \in c_5^*$ are mapped via μ_5^{-1} onto $P_5 \in b$ and $Q_5 \in a$.

It is the development engineer's job to deliver a spatial motion $\mu = \mu(t)$ interpolating the series S_i^* of the given window poses. The parameter t can be interpreted as a ‘*time parameter*’. Additionally, the motion μ is to slide the window S through the sealing slit (daylight curve c) with as little friction as possible.

To solve the task we first consider the displacements μ_i , $i = 0, \dots, n$, defined by $S \rightarrow S_i^*$. Clearly, the pre-images $P_i := \mu_i^{-1}(P_i^*)$ and $Q_i := \mu_i^{-1}(Q_i^*)$ of the points P_i^* and Q_i^* lie on the front boundary curve b and on the roofline curve a of S , respectively (Figure 2, left). Mind that not only the part of b between A and C and the part of a between B and C are involved but also the continuations beyond C . More detailed, we have: For $i = 0, \dots, n-2$ the points P_i on b lie between A and C and the points Q_i on a lie between B and C . For the vanishing position S_{n-1}^* we have $P_{n-1}^* = Q_{n-1}^*$ and $P_{n-1} = Q_{n-1} = C$ (Figure 2, left). For $i = n$ the points P_n and Q_n lie beyond the upper vertex C of S . In Figure 2, right, this position is highlighted.

In order to obtain an appropriate motion $\mu(t)$ we extract a minimal data set $[w_{b,i}, w_{a,i}, v_i, \beta_i] \in \mathbb{R}^4$ for each $i = 0, \dots, n$ representing the given position S_i^* . To this aim we first have to decompose each displacement μ_i in a canonic way (Section 2.1). In a second step we interpolate the constructed data $[w_{b,i}, w_{a,i}, v_i, \beta_i]$ by standard interpolation methods (Section 2.2).

2.1. Canonic decompositions of displacements μ_i

We want to decompose each of the given displacements μ_i

- into a displacement σ_i that gets P_i onto P_i^* and Q_i onto Q_i^* and additionally maintains the direction orthogonal to both lines P_iQ_i and $P_i^*Q_i^*$
- and into a subsequent rotation ρ_i about the axis $P_i^*Q_i^*$.

For $i = 0, \dots, n$, $i \neq n-1$, we define the unit vectors

$$\mathbf{e}_i := \pm \frac{\overrightarrow{P_iQ_i}}{\|\overrightarrow{P_iQ_i}\|} \quad \text{and} \quad \mathbf{e}_i^* := \pm \frac{\overrightarrow{P_i^*Q_i^*}}{\|\overrightarrow{P_i^*Q_i^*}\|}$$

where we take the positive signs if $0 \leq i < n-1$ and the negative signs if $i = n$.

In case of the vanishing position ($i = n-1$) where $P_{n-1} = Q_{n-1} = C$, $P_{n-1}^* = Q_{n-1}^*$ and hence, the vectors \mathbf{e}_{n-1} , \mathbf{e}_{n-1}^* cannot be defined by the formulae above, we instead put \mathbf{e}_{n-1} as angle bisector of the two adjacent directions \mathbf{e}_{n-2} and \mathbf{e}_n :

$$\mathbf{e}_{n-1} := \frac{\mathbf{e}_{n-2} + \mathbf{e}_n}{\|\mathbf{e}_{n-2} + \mathbf{e}_n\|}.$$

Then we compute \mathbf{e}_{n-1}^* as the corresponding direction of \mathbf{e}_{n-1} w.r.t. μ_{n-1} .

- If P_iQ_i and $P_i^*Q_i^*$ are not parallel the direction \mathbf{d}_i normal to both of them is defined by

$$\mathbf{d}_i := \frac{\mathbf{e}_i \times \mathbf{e}_i^*}{\|\mathbf{e}_i \times \mathbf{e}_i^*\|}. \quad (1)$$

In that case the displacement σ_i is determined by

$$\tilde{\mathbf{x}} := \mathbf{p}_i^* + \mathbf{M}_i \cdot (\mathbf{x} - \mathbf{p}_i) \quad (2)$$

where \mathbf{M}_i denotes the rotation matrix belonging to the axis direction \mathbf{d}_i and to the rotation angle α_i defined by

$$\cos \alpha_i := \langle \mathbf{e}_i, \mathbf{e}_i^* \rangle, \quad \sin \alpha_i := \|\mathbf{e}_i \times \mathbf{e}_i^*\|. \quad (3)$$

The vectors \mathbf{p}_i , \mathbf{p}_i^* , \mathbf{x} , $\tilde{\mathbf{x}}$ are the position vectors of the points P_i , P_i^* , an arbitrary point X and its image $\tilde{X} = \sigma_i(X)$ under σ_i .

- If — just in case — $P_i Q_i$ and $P_i^* Q_i^*$ are parallel² we set the matrix \mathbf{M}_i in (2) as the identity matrix. In that case σ_i is a pure translation.

The second displacement ρ_i is a rotation about the axis $P_i^* Q_i^*$ whose normalized direction vector is \mathbf{e}_i^* . The corresponding rotation angle β_i can be determined as follows:

Let \tilde{A}_i denote the image of A under σ_i , i.e., $\sigma_i(A) = \tilde{A}_i$. Then $\rho_i(\tilde{A}_i) = \mu_i(A) = A_i^*$. As ρ_i is a rotation about the axis $P_i^* Q_i^*$, the angle β_i occurs between the planes $P_i^* Q_i^* \tilde{A}_i$ and $P_i^* Q_i^* A_i^*$ and hence also between the normal vectors

$$\tilde{\mathbf{n}}_i := \frac{\mathbf{e}_i^* \times \overrightarrow{P_i^* \tilde{A}_i}}{\|\mathbf{e}_i^* \times \overrightarrow{P_i^* \tilde{A}_i}\|} \quad \text{and} \quad \mathbf{n}_i^* := \frac{\mathbf{e}_i^* \times \overrightarrow{P_i^* A_i^*}}{\|\mathbf{e}_i^* \times \overrightarrow{P_i^* A_i^*}\|}$$

of these two planes. We get

$$\cos \beta_i := \langle \tilde{\mathbf{n}}_i, \mathbf{n}_i^* \rangle \quad \text{and} \quad \sin \beta_i := \|\tilde{\mathbf{n}}_i \times \mathbf{n}_i^*\|. \quad (4)$$

Thus, the rotation ρ_i is given by

$$\mathbf{x}^* := \mathbf{p}_i^* + \mathbf{N}_i \cdot (\tilde{\mathbf{x}} - \mathbf{p}_i^*) \quad (5)$$

where \mathbf{N}_i denotes the rotation matrix belonging to the axis direction \mathbf{e}_i^* and to the rotation angle β_i defined by (4).

2.2. Construction of a window motion by standard interpolation techniques

Let the triangular window sheet S be described by the barycentric parameterization³

$$\mathbf{s}(u, v, w) = \begin{bmatrix} x(u, v, w) \\ y(u, v, w) \\ z(u, v, w) \end{bmatrix} \quad (6)$$

where the parameters u, v, w run in the triangular domain

$$\mathcal{D} := \{(u, v, w) \mid u, v, w \in [0, 1], u + v + w = 1\} \quad (7)$$

with the vertices $U(u = 1, v = 0, w = 0)$, $V(u = 0, v = 1, w = 0)$, $W(u = 0, v = 0, w = 1)$ and the edges $VW \dots (u = 0, v + w = 1)$, $WU \dots (v = 0, u + w = 1)$, and $UV \dots (w = 0, u + v = 1)$ (see Figure 3, left).

We take it that the curves a (roofline curve) and b (front boundary curve) are determined by $u = 0$ and $v = 0$, respectively. Due to the condition $u + v + w = 1$, we can use w as the running parameter on both, a and b : Note that $w = 0$ delivers the bottom points B and A of a and b whereas $w = 1$ yields the common point C of these two curves (Figure 3, right). In the same way we can assume that the daylight curve c is determined by $w = 0$ and the parameter v controls the points on c , where A and B belong to the parameters $v = 0$ and $v = 1$, respectively. These parameterizations of the boundary curves b , a and c read as:

$$b \dots \mathbf{b}(w) = \mathbf{s}(1 - w, 0, w), \quad (8)$$

$$a \dots \mathbf{a}(w) = \mathbf{s}(0, 1 - w, w), \quad (9)$$

$$c \dots \mathbf{c}(v) = \mathbf{s}(1 - v, v, 0). \quad (10)$$

²This also includes the case $i = 0$ where the two lines $P_i Q_i$ and $P_i^* Q_i^*$ are even identical!

³For barycentric coordinates see for example [1, p. 304–306], [5, p. 289–290], [4, p. 226–228].

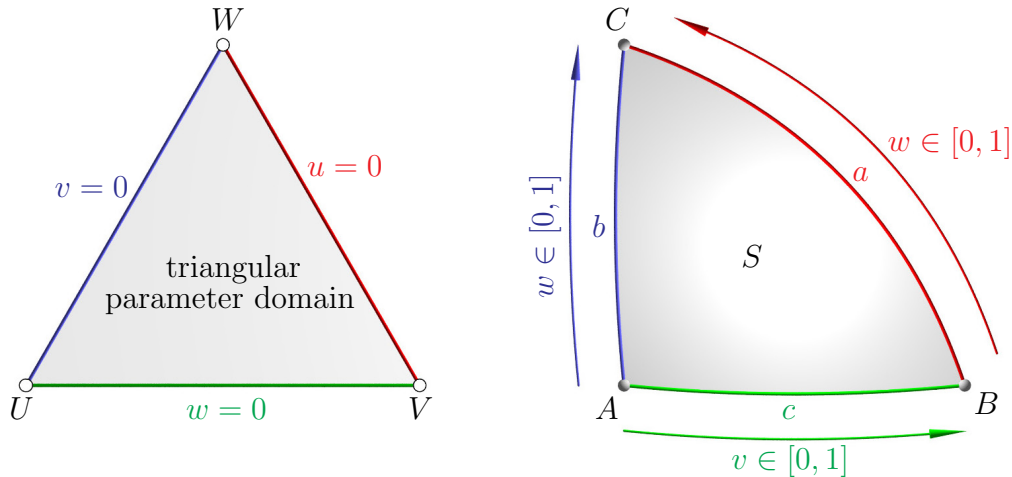


Figure 3: Barycentric parameterization of the window sheet.

Left: Parameter domain and its boundary lines: $u, v, w \in [0, 1]$, $u + v + w = 1$.

Right: The triangular surface with its boundary curves. Front boundary curve b (blue), roofline curve a (red), the daylight curve c , also representing the sealing slit (green).

Let $w_{b,i}$, $w_{a,i}$ and v_i be the parameter values belonging to the points P_i , Q_i and P_i^* w.r.t. the parameterizations (8), (9) and (10)

$$\mathbf{b}(w_{b,i}) = \mathbf{p}_i, \quad \mathbf{a}(w_{a,i}) = \mathbf{q}_i, \quad \mathbf{c}(v_i) = \mathbf{p}_i^*.$$

Then, together with the angles β_i (4) from the first step we obtain the $n + 1$ data quadruples $[w_{b,i}, w_{a,i}, v_i, \beta_i]^\top$ in \mathbb{R}^4 . We choose appropriate parameter values

$$t_0 = 0 < t_1 < \dots < t_{n-1} = 1 < t_n \in \mathbb{R}$$

and define a suitable interpolation curve

$$\mathbf{g}(t) = \begin{bmatrix} w_b(t) \\ w_a(t) \\ v(t) \\ \beta(t) \end{bmatrix}, \quad t \in [t_0, t_n]$$

satisfying

$$\mathbf{g}(t_i) = \begin{bmatrix} w_b(t_i) \\ w_a(t_i) \\ v(t_i) \\ \beta(t_i) \end{bmatrix} = \begin{bmatrix} w_{b,i} \\ w_{a,i} \\ v_i \\ \beta_i \end{bmatrix}.$$

As for the construction of interpolating spline curves see [4, p. 116 – 136].

Every point $\mathbf{g}(t)$ of this interpolation curve delivers — apart from the angle $\beta(t)$ — three parameters $w_b(t)$, $w_a(t)$ and $v(t)$ which, via (8), (9), (10)), yield three points $P \dots \mathbf{b}(w_b(t))$, $Q \dots \mathbf{a}(w_a(t))$ and $P^* \dots \mathbf{c}(v(t))$ on the boundary curves b , a and c of S , respectively. Having found P , Q and P^* it is easy to determine the appropriate⁴ point $Q^* \in c$ such that

$$\text{dist}(P^*, Q^*) = \text{dist}(P, Q).$$

⁴The values of t lying in the interval $]0, t_{n-1} = 1[$ correspond to the positions of Q^* lying between P^* and B whereas the values t in $]t_{n-1} = 1, t_n[$ belong to points Q^* between P^* and A .

The motion $\mu(t)$ is now constructed in the following way: For each instant t we compose

- the displacement $\sigma(t)$ that brings P into P^* and Q into Q^* and maintains the direction normal to both lines PQ and P^*Q^*
- and the rotation $\rho(t)$ with angle $\beta(t)$ about the axis P^*Q^* .

To determine the first transformation $\sigma = \sigma(t)$ we only need to follow the recipe of Section 2.1. We just have to replace the points P_i, Q_i, P_i^*, Q_i^* by the points P, Q, P^*, Q^* to obtain the direction vector $\mathbf{d} = \mathbf{d}(t)$ and the angle $\alpha = \alpha(t)$ that constitute the rotation matrix $\mathbf{M}(t)$. The transformation $\sigma(t)$ is then given by

$$\tilde{\mathbf{x}} := \mathbf{p}^* + \mathbf{M} \cdot (\mathbf{x} - \mathbf{p}). \quad (11)$$

The second displacement $\rho = \rho(t)$ is a rotation about the axis P^*Q^* ; the axis direction is

$$\mathbf{e}^* := \pm \frac{\overrightarrow{P^*Q^*}}{\|\overrightarrow{P^*Q^*}\|}.$$

We choose the positive leading sign if Q^* lies between P^* and B and the negative leading sign if Q^* lies between P^* and A . The rotation angle is $\beta(t)$; together with $\mathbf{e}^*(t)$ it defines the rotation matrix $\mathbf{N}(t)$. The emerging rotation $\rho(t)$ reads as

$$\mathbf{x}^* := \mathbf{p}^* + \mathbf{N} \cdot (\tilde{\mathbf{x}} - \mathbf{p}^*). \quad (12)$$

Finally, the composition of $\sigma(t)$ and $\rho(t)$ (substitution of (11) into (12)) gets us the resulting motion $\mu(t) = \rho(t) \circ \sigma(t)$

$$\mathbf{x}^* := \mathbf{p}^* + \mathbf{N} \cdot \mathbf{M} \cdot (\mathbf{x} - \mathbf{p}). \quad (13)$$

Note that the presented recipe only fails if $t = t_{n-1} = 1$ (or numerically if t is *very close to* 1), i.e., when we happen to deal with the vanishing position S_{n-1}^* of the window S . In that instance we have $P = Q = C$ and $P^* = Q^*$ which is why the vectors \mathbf{d} and \mathbf{e}^* cannot be computed as described above. Instead, we simply put: $\mu(t) = \mu(t_{n-1}) = \mu(1)$.

Result 1. *Let a triangular window sheet S with the parameterization (6), its roofline curve a , its front boundary curve b and its daylight curve c be given. Let moreover $S_i^*, i = 0, \dots, n$, be a series of prescribed positions of S such that $S_0^* = S$ and, for $i = 0, \dots, n$, the front boundary curve b_i^* and the roofline curve a_i^* of S_i^* meet the daylight curve c of S in points P_i^* and Q_i^* , respectively. Then the motion μ given by the representation (13) moves S in a way that*

- the prescribed positions S_i^* are assumed and
- at any point in time t the front boundary curve $\mu(b)$ and the roofline curve $\mu(a)$ of $\mu(S)$ intersect the daylight curve c in two points $P^*(t)$ and $Q^*(t)$.

3. A kinematic surface as a possible substitute

We have stated above that *sliding the window through the daylight curve c amounts to slipping c across the window surface*. This observation is crucial as it encourages us to construct a substitute window surface: If we subject the daylight curve c to the inverse $\mu^{-1}(t)$ of the window retraction motion $\mu(t)$ we obtain a kinematic surface S_c that is close to the initial

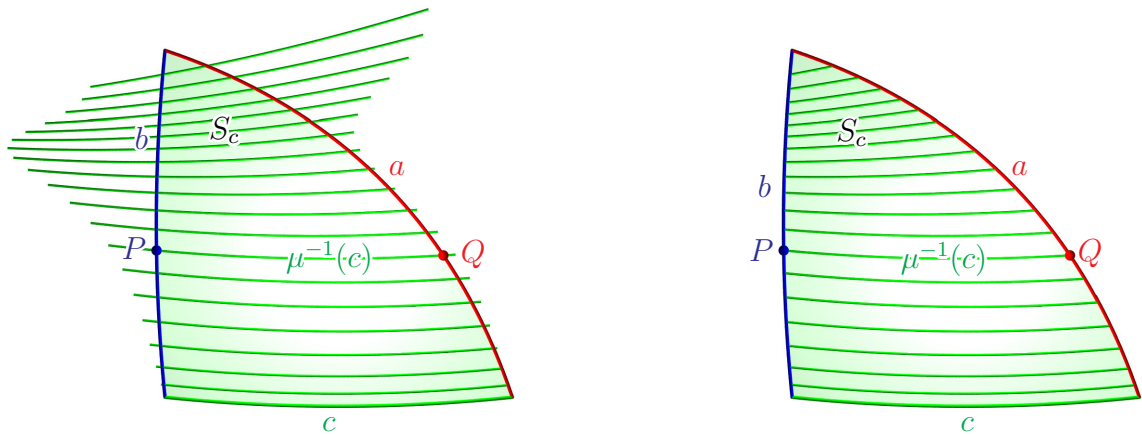


Figure 4: **Left:** The daylight curve c subjected to the inverse of the window motion μ generates a kinematic surface S_c .

Right: Obviously, the emerging geometric surface has to be trimmed along the given boundary curves a and b .

surface S (Figure 4, left). As $\mu(t)$ guides both, the front boundary curve b and the roofline curve a such that they — at any point in time t — intersect the daylight curve c in two respective points P^*, Q^* , the inverse motion $\mu^{-1}(t)$ moves c in a way that its instances always meet b and a in two points P and Q . In other words: The two surfaces S and S_c have the three boundary curves b, a and c in common. Of course, only the part of S_c within these boundary curves is what we are interested in. The only thing that is left to be done is trimming S_c along the given boundary curves a and b (Figure 4, right).

Result 2. *The described construction generates a patch contained in a kinematic surface S_c . The surface S_c can be generated by the inverse $\mu^{-1}(t)$ of the window retraction motion $\mu(t)$ applied to the daylight curve c . The surface patch S_c and the surface S share their boundary curves b, a and c . If we apply the motion $\mu(t)$ to the surface S_c we obtain a continuous series $S_c(t)$ of positions each of them containing the daylight curve c . This means that the patch S_c perfectly slides through the sealing slit without any deflection.*

The parameterization arising from the generation as a kinematic surface, however, is unfavorable for our further computations. An appropriate parameterization of this part of S_c can be obtained by means of projection: Starting with the parameterization (6) of S we get a barycentric parameterization $\mathbf{s}_c(u, v, w)$

$$\mathbf{s}_c(u, v, w) = \begin{bmatrix} x_c(u, v, w) \\ y_c(u, v, w) \\ z_c(u, v, w) \end{bmatrix}, \quad u + v + w = 1, \quad u, v, w \in [0, 1] \tag{14}$$

of S_c by orthogonally projecting the points of S onto S_c : For each point $X \dots \mathbf{s}(u, v, w)$ on S the image point $X_c \dots \mathbf{s}_c(u, v, w)$ is defined as the pedal point⁵ of X on S_c . This implies that the parameterizations (8), (9) and (10) of the common boundary curves b, a, c of S and S_c

⁵If S and S_c are sufficiently close the orthogonal projection from S to S_c is a well-defined and bijective mapping.

are now parameterized identically:

$$\begin{aligned} b \dots \mathbf{b} &= \mathbf{b}(w) = \mathbf{s}(1-w, 0, w) = \mathbf{s}_c(1-w, 0, w), \\ a \dots \mathbf{a} &= \mathbf{a}(w) = \mathbf{s}(0, 1-w, w) = \mathbf{s}_c(0, 1-w, w), \\ c \dots \mathbf{c} &= \mathbf{c}(v) = \mathbf{s}(1-v, v, 0) = \mathbf{s}_c(1-v, v, 0). \end{aligned}$$

4. A family of alternatives

Having constructed the spatial motion $\mu(t)$ we can now examine the given window surface S in the course of its motion. We concentrate on the sealing slit along the daylight curve c where S has to pass through. Obviously, as S is not a kinematic surface with respect to μ^{-1} generated by c it will not slide through c without any deviation. The motion $\mu(t)$ drives S in a way that its front boundary curve b and its roofline curve a meet c all the way down on its path. But still, we cannot be sure that unwanted deviations and friction appear in the course of the motion $\mu(t)$.

On the other hand, the kinematic surface S_c constructed in Section 3 can in fact be moved through c under the motion $\mu(t)$ without any deflection. So, comparing the given window sheet S to S_c and measuring their distances enables the engineer to assess the quality of S . The maximum distance δ of S and S_c directly relates⁶ to the stress exerted to the sealing along c while S is moved w.r.t. $\mu(t)$. Obviously, $\delta = 0$ amounts to $S = S_c$.

Unsurprisingly, the following question arises: Why don't we substitute S by S_c in the first place? The reason why we do not do so right away is that replacing the stylist's window sheet S by another surface is a delicate issue. In order to leave the final judgement at the discretion of the development engineer we set up a tool such that he or she can allow for the laws of physics (including the constraints of the sealing manufacturer) and still keep the stylist happy:

- We create a family $\{S_f\}$ of surfaces whose members are very close to the given surface S , all the more so in the areas near the boundary curves. This way we can avoid disturbing the visual continuity towards neighbouring surfaces. Any interference of the overall impression is marginal if negligible.
- The surfaces of $\{S_f\}$ will cause a smaller maximum distance δ_f to S and, consequently, reduce the friction along the sealing slit c when they are subjected to the retraction motion $\mu(t)$.
- Additionally we offer a number of parameters controlling the remaining distance δ_f and the degrees of smoothness w.r.t. S along the boundary curves.

To obtain these intermediate surfaces S_f between S and S_c we use a certain polynomial blending function f :

Definition 1. *Let k, l, m be non-negative integers and let d_0 be a real value in the interval $[0, 1]$; then we define the function*

$$f(u, v, w) := d u^k v^l w^m \tag{15}$$

on the triangular parameter domain \mathcal{D} given by (7). The constant d is given by

$$d := \frac{(k+l+m)^{k+l+m}}{k^k l^l m^m} \cdot d_0.$$

⁶For practical applications the maximum distance δ can be viewed as a measure for the stress exerted to the sealings.

Proposition 1. *The function $f(u, v, w)$ has the following properties:*

(a) If $\begin{cases} k > 0 \\ l > 0 \\ m > 0 \end{cases}$ then $\begin{cases} \forall w : f(0, 1 - w, w) = 0 \\ \forall w : f(1 - w, 0, w) = 0 \\ \forall v : f(1 - v, v, 0) = 0 \end{cases}$.

(b) If $\begin{cases} k > 0 \\ l > 0 \\ m > 0 \end{cases}$ all partial derivatives of $f(u, v, w)$ w.r.t. u, v, w of order $i \leq \begin{cases} k - 1 \\ l - 1 \\ m - 1 \end{cases}$

along the boundary edges $\begin{cases} VW : u = 0, v + w = 1 \\ WU : v = 0, u + w = 1 \\ UV : w = 0, u + v = 1 \end{cases}$ of the triangular parameter domain \mathcal{D} vanish.

- (c)
 - If $k = l = m = 0$ then f is the constant function $f(u, v, w) \equiv d_0$.
 - If $d_0 \neq 0$ and at least one of the non-negative integers k, l, m is different from zero, then the values of f in the triangular domain \mathcal{D} vary in the interval $[0, d_0]$. In the interior of \mathcal{D} , i.e., for $u, v, w \in]0, 1[; u + v + w = 1$ the function f has only positive values in the interval $]0, d_0]$. In that case f assumes the maximum value d_0 in \mathcal{D} at

$$(u_0, v_0, w_0) = \left(\frac{k}{k+l+m}, \frac{l}{k+l+m}, \frac{m}{k+l+m} \right). \tag{16}$$

Proof. (a) and (b) are obvious consequences of Definition 1.

(c) Let Φ denote the graph of the function f . The statement for $k = l = m = 0$ is again trivial. Let now $d_0 \neq 0$ and let at least one of the values k, l, m be different from zero. Then, as one can easily verify, the value of f at (u_0, v_0, w_0) is indeed d_0 . To show that this is the maximum value of f in the triangular domain \mathcal{D} we have to distinguish three cases:

- If only one of the three values k, l, m is different from zero, say $k = l = 0$ and $m > 0$, we have

$$f(u, v, w) = d w^m = d (1 - u - v)^m.$$

Obviously, the function graph Φ of f is a cylinder surface whose generators are parallel to the edge UV of the parameter triangle \mathcal{D} (Figure 5, left). Clearly, in this case, the

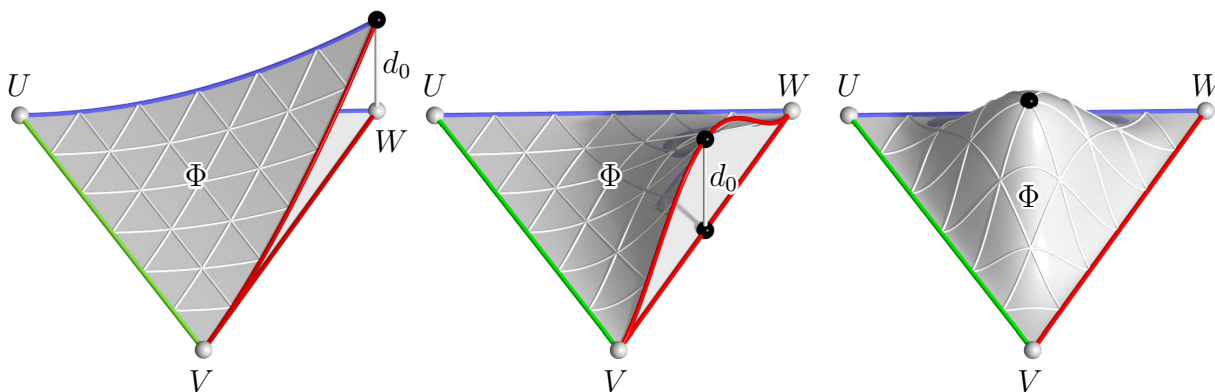


Figure 5: Function graph Φ for the following cases:
Left: $k = l = 0, m = 2$. **Center:** $k = 0, l = m = 2$. **Right:** $k = l = m = 2$.

maximum of f in the domain \mathcal{D} is reached at the third vertex $W(u_0 = v_0 = 0, w_0 = 1)$ of \mathcal{D} and has the value d_0 .

- If two of the values k, l, m are non-zero whereas the third vanishes, say $k = 0$ and $l, m > 0$, we have

$$f(u, v, w) = d v^l w^m. \quad (17)$$

Along the edges WU and UV of the parameter triangle \mathcal{D} and nowhere else we have $f(u, v, w) = 0$. Moreover, the two partial derivatives

$$\frac{\partial f}{\partial v} = d l v^{l-1} w^m, \quad \frac{\partial f}{\partial w} = d m v^l w^{m-1}$$

can vanish simultaneously only along these edges WU and UV . This shows that the maximum must occur in a point of the remaining edge VW of the triangular domain \mathcal{D} ; i.e., the maximum is a point on the intersection curve of the graph Φ of f with the vertical plane through VW (Figure 5, center). This curve is obtained by substitution of $u = 0$, i.e., $w = 1 - v$ into (17):

$$f(0, 1 - w, w) = d (1 - w)^l w^m.$$

One can easily check that this univariate function assumes its maximum at $w = w_0 = \frac{m}{l+m}$. Substitution into $v_0 = 1 - w_0$ yields $v = v_0 = \frac{l}{l+m}$ which finishes the proof in that case.

- In the remaining case ($k, l, m > 0$) the function f is zero all along the three edges UV , VW , WU of the parameter domain \mathcal{D} (Figure 5, right). As f has only positive values in the interior of \mathcal{D} the maximum value of f must be assumed there. To determine this maximum we substitute $w = 1 - u - v$ into (15) and compute the first partial derivatives with respect to u and v :

$$\begin{aligned} \frac{\partial f}{\partial u} &= d u^{k-1} v^l (1 - u - v)^{m-1} \cdot [k - (m+k)u - kv], \\ \frac{\partial f}{\partial v} &= d u^k v^{l-1} (1 - u - v)^{m-1} \cdot [l - lu - (m+l)v]. \end{aligned}$$

Hence, the condition for the maximum is the pair of linear equations

$$\begin{aligned} (k+m)u + kv &= k, \\ lu + (l+m)v &= l \end{aligned}$$

whose solution turns out to be $u_0 = \frac{k}{k+l+m}$, $v_0 = \frac{l}{k+l+m}$. Adding $w_0 = 1 - u_0 - v_0 = \frac{m}{k+l+m}$ finally delivers (16). \square

Let now $d_0 \in [0, 1]$ and k, l, m be non-negative integers. We define blending surfaces $S_f = S_f(k, l, m, d_0)$ via

$$S_f \dots \mathbf{s}_f(u, v, w) := \mathbf{s}(u, v, w) + f(u, v, w) \cdot (\mathbf{s}_c(u, v, w) - \mathbf{s}(u, v, w)). \quad (18)$$

Every choice of d_0 and k, l, m provides an instance of S_f .

Proposition 2. *The surface $S_f \dots \mathbf{x}_i(u, v, w)$ has the following properties:*

- (a) S_f shares its boundary curves b, a, c with S and S_c .
- (b) All partial derivatives of $\mathbf{s}(u, v, w)$ and $\mathbf{s}_f(u, v, w)$ w.r.t. u, v, w of order $i \leq \begin{cases} k \\ l \\ m \end{cases}$ along the boundary curve $\begin{cases} b \dots \mathbf{b}(w) = \mathbf{s}(1-w, v=0, w) \\ a \dots \mathbf{a}(w) = \mathbf{s}(u=0, 1-w, w) \\ c \dots \mathbf{d}(v) = \mathbf{s}(1-v, v, w=0) \end{cases}$ are identical.
- (c) S_f is contained in the convex domain spanned by S and S_c .
- (d) The surface $\begin{cases} S \\ S_c \end{cases}$ is contained in the set $\{S_f\}$ for $\begin{cases} d_0 = 0, \\ k = l = m = 0, d_0 = 1. \end{cases}$
- (e) If δ denotes the maximum distance between the surfaces S and S_c then the maximum distance δ_f between S_f and S will not exceed the value $d_0 \delta$.

Remarks:

- (a) Proposition 2, (b) signifies that for $k = 1$ the surfaces S_f and S are tangent all along the roof curve a . For $k \geq 2$ the two surfaces are even curvature continuous along a . Analogous properties can be stated for the other boundary curves b and c and the integers l and m , respectively.
- (b) For fair surfaces as used in our practical case Proposition 2, (c) means that S_f is contained in the spatial domain bounded by S and S_c .
- (c) If especially $k = l = m$ then $u_0 = v_0 = w_0 = \frac{1}{3}$ and the maximum deviation of S and S_f belongs to the barycenter of the triangular parameter domain \mathcal{D} .

Proof of Proposition 2.

- (a) follows from the definition (18) of S_f as S and S_c have common boundary curves.
- (b) We exemplarily restrict the proof to the boundary curve (roofline curve) a ($u = 0, v + w = 1$). For $i \leq k$ and $i_1, i_2, i_3 \in \mathbb{N}_0$ with $i_1 + i_2 + i_3 = i$ we apply the product rule of differentiation and obtain

$$\begin{aligned} \frac{\partial^i \mathbf{s}_f}{(\partial u)^{i_1} (\partial v)^{i_2} (\partial w)^{i_3}} &= \frac{\partial^i \mathbf{s}}{(\partial u)^{i_1} (\partial v)^{i_2} (\partial w)^{i_3}} + \frac{\partial^i f}{(\partial u)^{i_1} (\partial v)^{i_2} (\partial w)^{i_3}} \cdot \overbrace{(\mathbf{s}_c - \mathbf{s})}^{(*)} + \\ &+ \sum_{j_1+j_2+j_3 < i} c_{j_1, j_2, j_3} \cdot \underbrace{\frac{\partial^{j_1+j_2+j_3} f}{(\partial u)^{j_1} (\partial v)^{j_2} (\partial w)^{j_3}}}_{(**)} \cdot \frac{\partial^{i-(j_1+j_2+j_3)} (\mathbf{s}_c - \mathbf{s})}{(\partial u)^{i_1-j_1} (\partial v)^{i_2-j_2} (\partial w)^{i_3-j_3}}, \end{aligned}$$

where c_{j_1, j_2, j_3} are certain constants in \mathbb{N}_0 .

According to the preconditions we have $\mathbf{s}_c = \mathbf{s}$ all along the roofline curve a , i.e., $(*) = 0$. Due to Proposition 1, (b) all partial derivatives of f of order $< k$ vanish, and so does $(**)$. Thus,

$$\frac{\partial^i \mathbf{s}_f}{(\partial u)^{i_1} (\partial v)^{i_2} (\partial w)^{i_3}} = \frac{\partial^i \mathbf{s}}{(\partial u)^{i_1} (\partial v)^{i_2} (\partial w)^{i_3}}$$

holds all along the boundary curve a .

- (c) follows from the fact that the blending function f only assumes values in the interval

[0, 1].

(d) can easily be verified by substitution of the given values of d_0, k, l, m .

(e) We have:

$$\delta_f = \max_{u,v,w} \{\|s_f - s\|\} = \max_{u,v,w} \{f \cdot \|s_c - s\|\} \leq \overbrace{\max_{u,v,w} \{f\}}^{=d_0} \cdot \overbrace{\max_{u,v,w} \{\|s_c - s\|\}}^{=\delta} = d_0 \cdot \delta \quad \square$$

Remark: The figure δ is a measure for the deviation of S along the daylight curve c . If δ exceeds the allowed limits of deviation we can choose an appropriate d_0 in $]0, 1[$ and replace S by one of the respective surface S_f . The maximum distance δ_f of S_f and S does not exceed the value $d_0\delta$ according to Proposition 2, (e). Choosing $d_0 = 1$ and $k = l = m = 0$ amounts to replacing S by S_c and hence to avoiding any deviation along the sealing. Any choice of d_0 in $[0, 1]$ will diminish the deviation to a value between δ and 0. The choice of d_0 provides a handy tool for the control of the friction. Simultaneously, the choice of k, l, m neatly controls the shape of the replacement surface S_f along the boundary curves.

5. Conclusions

A couple of decades ago side window panes were mostly flat. In those times a simple vertical shift could do the job of moving the window up or down. Now, that the car windows are curved the job of computing an appropriate spatial motion to properly shift the window has gradually become an issue. This is why the problem of moving car windows has been addressed in a number of papers within the last few years.

Rear side windows of convertibles (cabriolets) often have to be moved in a very sophisticated way. There are additional constraints to be observed: On the one hand, spatial limitations demand that a set of predetermined positions be assumed. On the other hand, though, the surface has to be moved through the sealing slit. In this paper we tried to present a recipe how these conditions can both be met. This recipe intends to put the designer into the position to create a suitable spatial motion for the rear side window of a cabriolet that moves the window sheet from its closed position down to the position where the whole window is hidden inside the car side panel.

We started our considerations with a given rear side window and a set of predefined positions of the desired motion. To further improve the process it would be a promising approach to preprocess the whole design. While selecting the set of further positions the engineer exerts great influence on the final result. We would like to enable the engineer to act wilfully in this early stage of the process. The tool to do so is yet to be designed.

It would be a great step forward if such considerations were already in the stylists' mind. Such a step of integration would considerably accelerate car development and engineering.

References

- [1] G. FARIN: *Curves and Surfaces for Computer Aided Geometric Design*. Academic Press, Boston 1990.
- [2] A. GFERRER, J. LANG, A. HARRICH, M. HIRZ, J. MAYR: *Car side window kinematics*. *Computer-Aided Design* **43**, 410–416 (2011).

- [3] A. HARRICH, J. MAYR, M. HIRZ, P. ROSSBACHER, J. LANG, A. GFRERRER, A. HASELWANTER: *CAD-based synthesis of a window lifter mechanism*. SAE World Congress, Detroit 2010.
- [4] M. HIRZ, W. DIETRICH, A. GFRERRER, J. LANG: *Integrated Computer-Aided Design in Automotive Development*. Springer, Heidelberg 2013.
- [5] J. HOSCHEK, D. LASSER: *Fundamentals of Computer Aided Geometric Design*. A K Peters, Wellesley Massachusetts 1993.
- [6] H. WEBER: *Scheibeführung für eine absenkbare sphärisch gekrümmte Fensterscheibe in einer Fahrzeugtür*. Patentschrift DE 195 04 781 C1, 22.08.1996, Deutsches Patentamt, 1996.

Received September 22, 2015; final form March 31, 2016